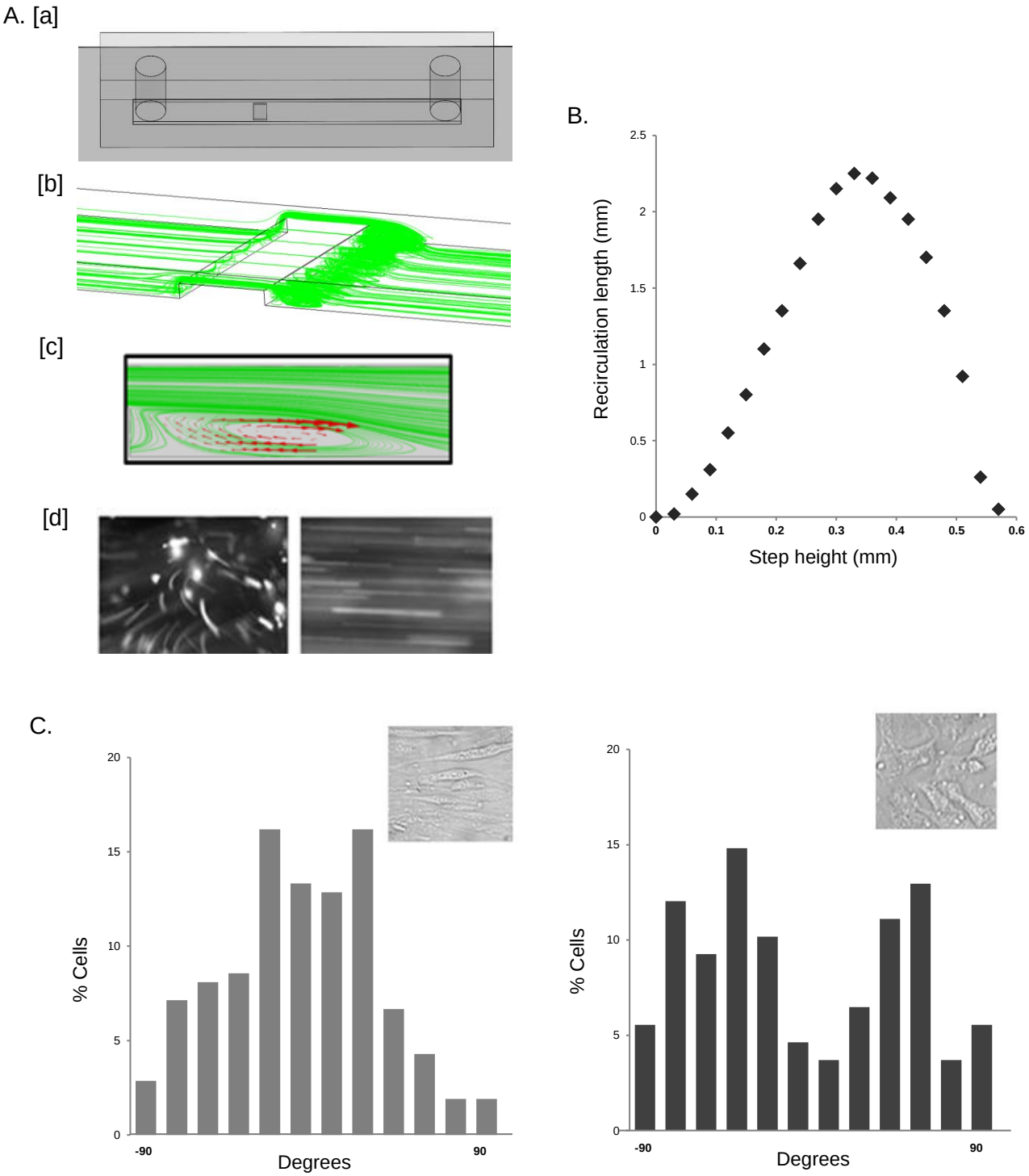

Supplemental Figure I: ***A:*** **[a]** CAD (computer aided design) image of the final chamber design depicting the step barrier midway in the chamber and fluid inlet/outlet on each side. **[b]** Computational fluid dynamics (CFD) simulation showing the streamlines of a recirculation region following a step barrier and unidirectional laminar flow before and after the step. **[c]** Streamlines (green) and velocity vectors (red) depicting the recirculating, disturbed flow patterns after the step barrier. **[d]** The trajectories of fluorescent microbeads under flow after the step (left) compared to the laminar region. ***B:*** Recirculation length after the step barrier as a function of varying step height. ***C:*** Endothelial alignment measurements in HAECs in LF (left) and DF conditions. 20-40 cells per condition, n=3 independent experiments. Inset shows representative images of the characteristic endothelial morphology of HAECs under LF (left) and DF.

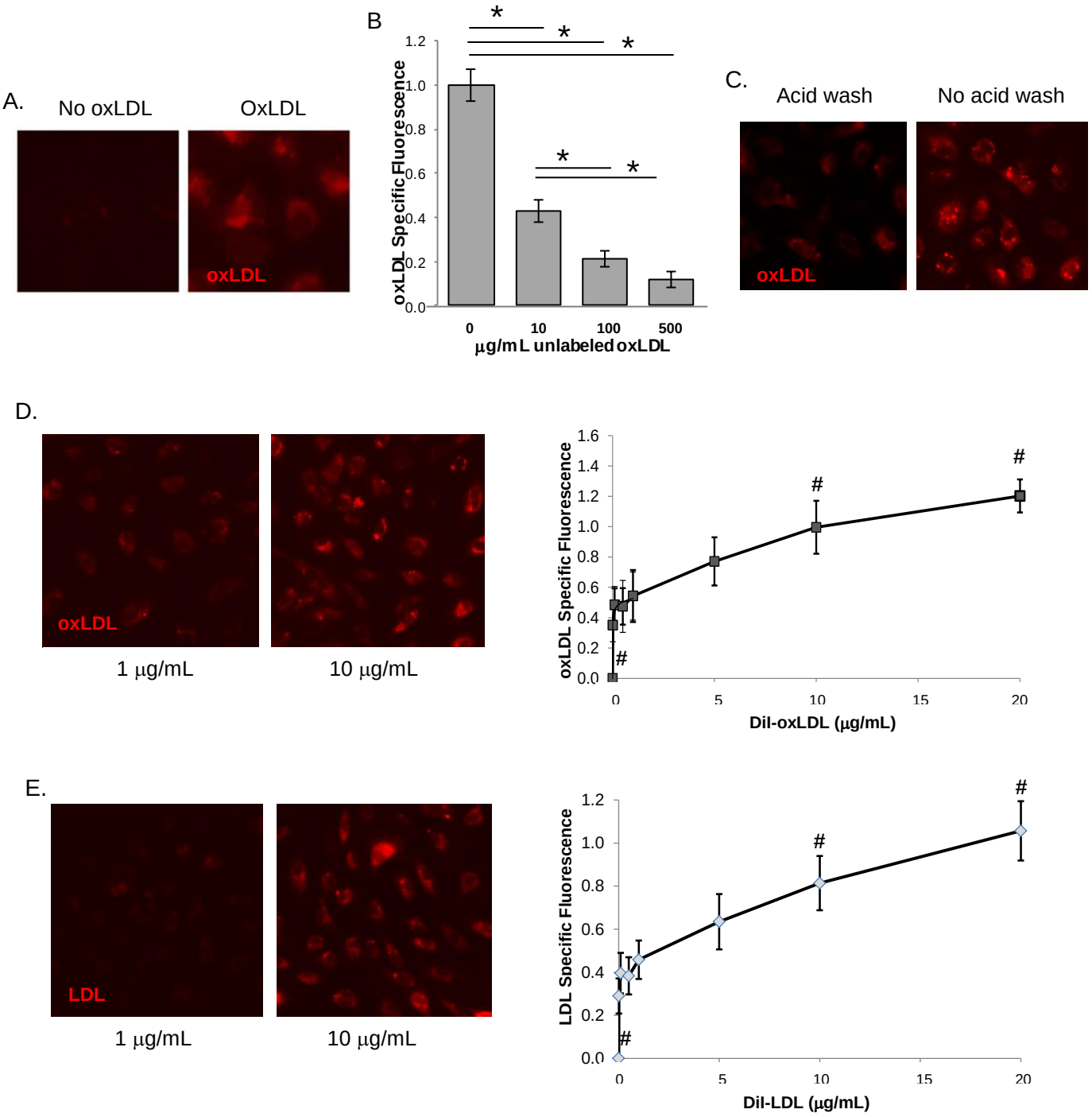

Supplemental Figure II: ***A:*** Representative rhodamine images of cells without DiI-oxLDL (left) and with DiI-oxLDL (right). ***B:*** OxLDL specific fluorescence as a function of the addition of increasing amounts of unlabeled oxLDL. ***C:*** Representative images visually show that an acid wash removes the undesired bound DiI-oxLDL particles still attached to the fixed ECs. ***D and E:*** OxLDL ***(D)*** and LDL ***(E)*** specific fluorescent signal as a function of increasing amounts of DiI-oxLDL and DiI-LDL, respectively. Representative images are shown on the left. * $p<0.05$; #$p<0.05$ with 1000 ng/mL DiI-oxLDL and DiI-LDL, respectively.

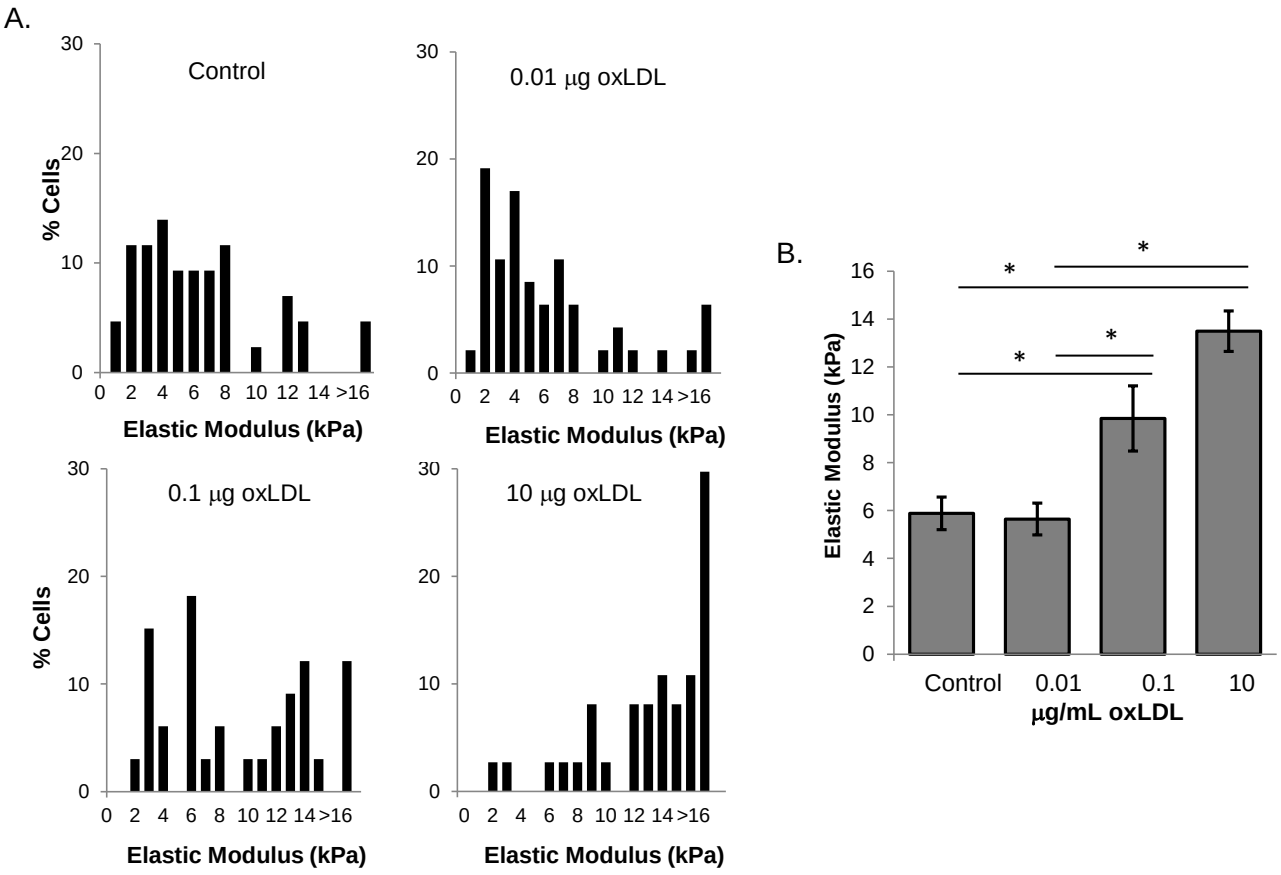

Supplemental Figure III: ***A:*** Histograms showing the elastic modulus values of HAECs exposed to varying concentrations of oxLDL for 48 hours. ***B:*** Average elastic modulus of HAECs treated with 0, 0.01, 0.1 or 10 μg/mL oxLDL. * $p<0.05$

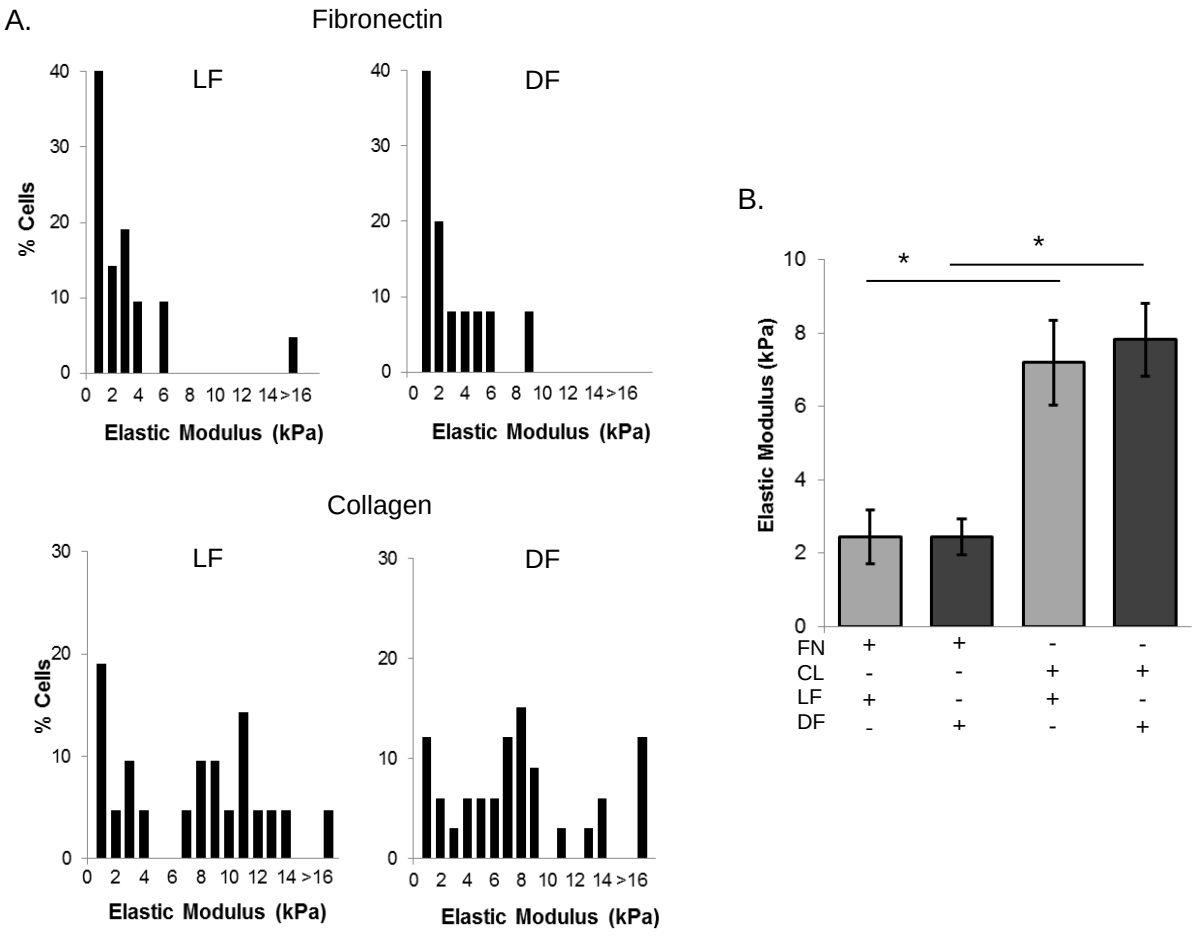

Supplemental Figure IV: ***A:*** Histograms depicting the elastic modulus of HAECs grown on fibronectin- (FN, top) and collagen-coated (CL, bottom) PDMS microfluidic devices following 48 hours of LF (left) and DF (right) (20-30 cells per condition, 4 independent experiments). ***B:*** Average elastic modulus of ECs from the above described conditions. * $p<0.05$.

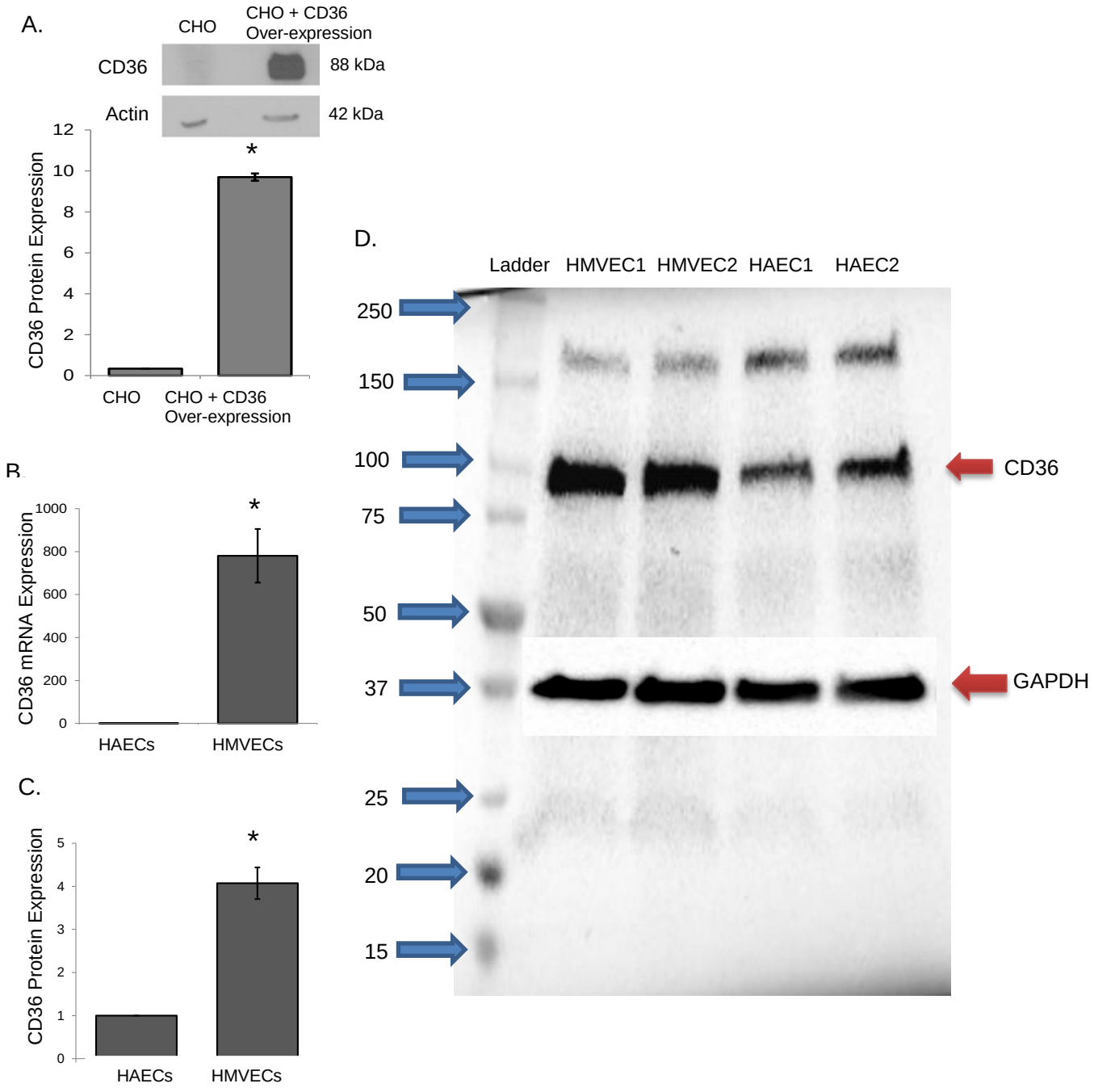

Supplemental Figure V: ***A:*** Representative western blot and average CD36 protein expression in CHO cells that do not express detectable amount of CD36 and CHO cells over-expressed with human CD36 construct (n=4). ***B, C and D:*** Average CD36 mRNA (n=3) ***(B)*** and protein expression (n=4) ***(C)*** in HAECs compared to HMVECs with representative full western blot gel with markers ***(D)***. *p<0.05

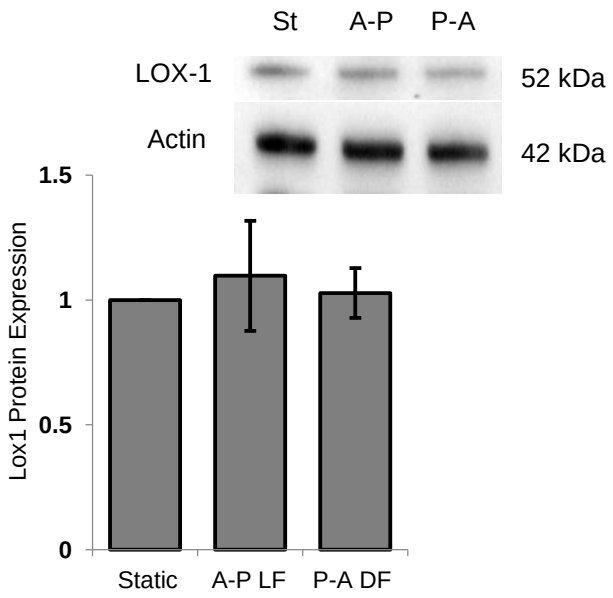

Supplemental Figure VI: Lox1 protein expression in HAECs exposed to 48 hours of athero-protective and pro-atherogenic flow as well as static conditions (n=5).

A.

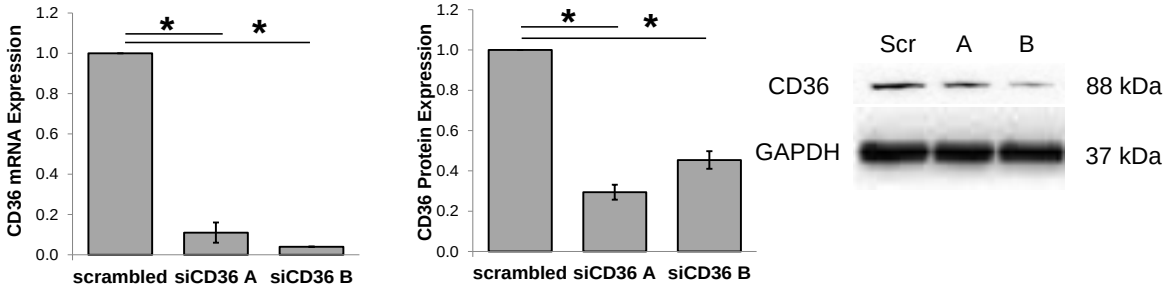

B.

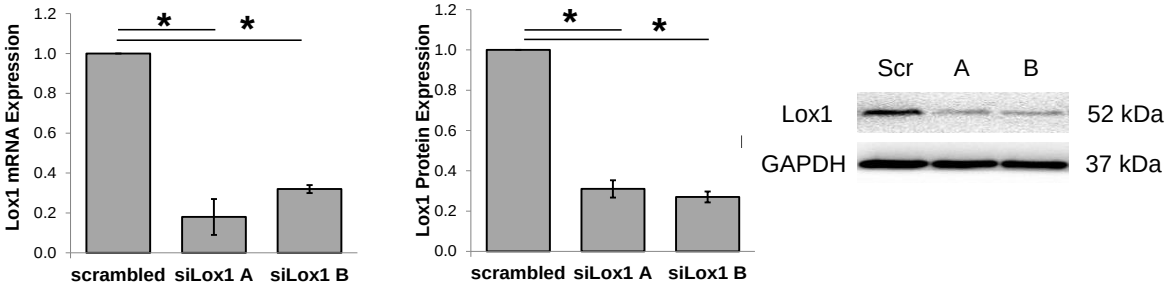

Supplemental Figure VII: ***A:*** CD36 mRNA expression (left) and CD36 protein expression (middle, right) for scrambled and two different CD36-targetting siRNAs. ***B:*** Lox1 mRNA expression (left) and Lox1 protein expression (middle, right) for scrambled and two different Lox1-targetting siRNAs.
***** $p<0.05$.

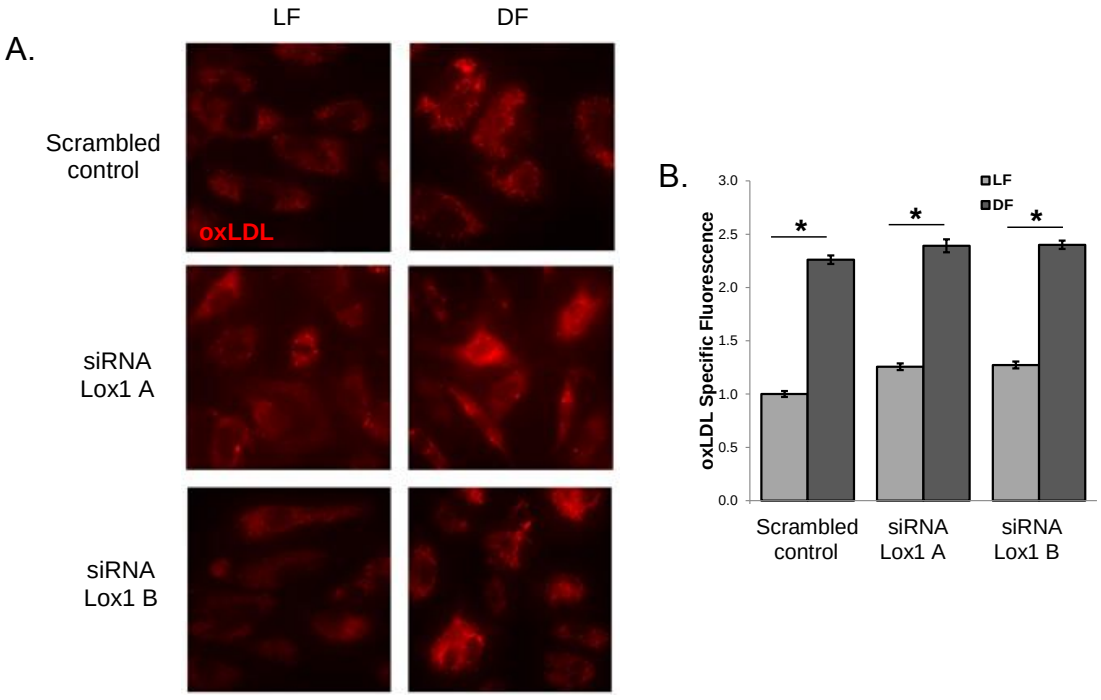

Supplemental Figure VIII: ***A:*** Representative images of DiI-oxLDL uptake into HAECs transfected with control (top) or Lox1-targetting siRNAs (middle, bottom) exposed to LF (left) and DF (right). ***B:*** Average oxLDL uptake into HAECs transfected with scrambled control or two different Lox1-targetted siRNAs under LF and DF conditions. 20-40 cells per condition per experiment, n=4 independent experiments ($p<0.05$).

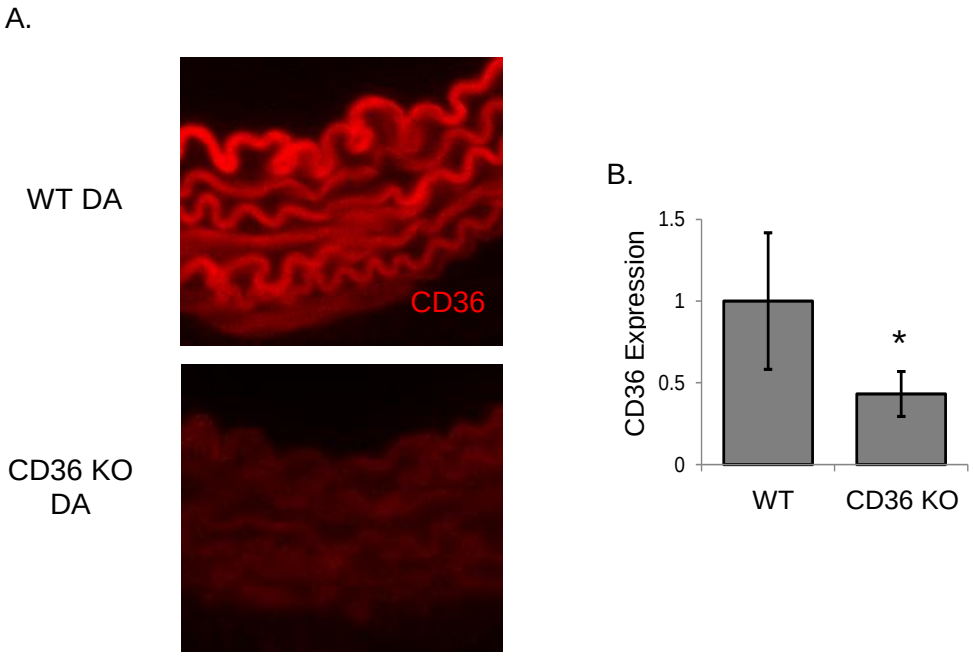

Supplemental Figure IX: ***A:*** Representative histology sections of descending aortic (DA) from WT (top) and CD36 KO (bottom) mice stained for CD36. ***B:*** Average CD36 expression in aortic sections from WT and CD36 KO mice (n=4, 15-20 sections per condition). * $p<0.05$.